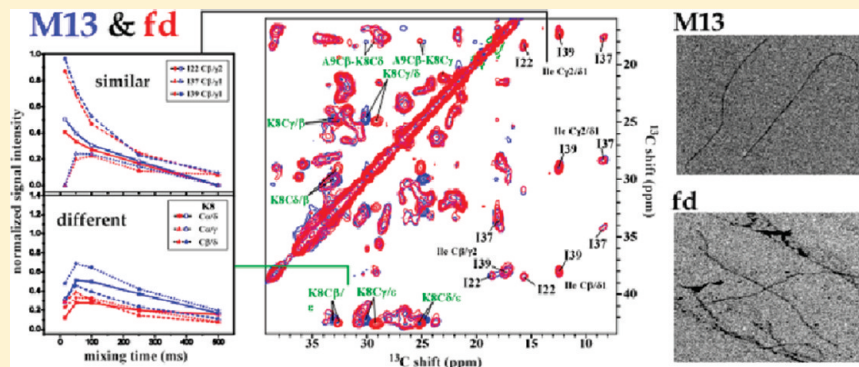


Similarities and Differences within Members of the Ff Family of Filamentous Bacteriophage Viruses

Omry Morag, Gili Abramov, and Amir Goldbourt*

Raymond and Beverly Sackler Faculty of Exact Sciences, School of Chemistry, Tel Aviv University, Ramat Aviv 69978, Tel Aviv, Israel

Supporting Information

ABSTRACT:

The filamentous bacteriophage viruses of the Ff family, fd and M13, slightly differ in their genome, and their 50-residue-long major capsid proteins have a single site difference: the uncharged asparagine-12 in M13 is replaced with a negatively charged aspartate in fd. We have used magic-angle spinning solid-state NMR spectroscopy to site-specifically assign the resonances belonging to the capsid protein of M13. Assignment of several mobile residues was facilitated by using J-based spectroscopy, which in addition provided sugar-base contacts in the M13-DNA stemming from two-bond scalar couplings. A comparison between M13 and fd bacteriophages reveals that the two virions have a very conserved and stable structure, manifested in negligibly small chemical shift differences and similar dynamic properties for nearly all resonances. The principal difference between the two phages involves residues in the vicinity of residue 12. We suggest that the elimination of the single charge at position 12 throughout the entire assembly affects the electrostatic and hydrogen-bonding interaction network governing inter- and intraresidue contacts, mainly by the rearrangement of the positively charged lysine residue at position 8.

INTRODUCTION

Filamentous bacteriophages (Inoviruses¹) comprise a family of virions that have only about 10 genes and grow in specific hosts. M13, fd, and f1 (generally referred to as Ff) are very similar inoviruses having a single-stranded circular DNA molecule packaged inside a capsid that consists of several thousands of copies of identical coat protein subunits. A few other proteins cap both ends of the virion and are specific for the infection and assembly processes. The relative simplicity of these viruses and the ease with which they can be genetically manipulated has made them ideal systems for a large range of applications such as phage display,^{2,3} DNA cloning and sequencing,^{4,5} nanomaterial fabrication,⁶ and drug-carrying nanomachines.^{7–10} The unique elongated fibrous shape of bacteriophages and their mostly helical molecular structure (of both capsid and DNA) has also made them ideal candidates for studies of liquid-crystal formation.^{11–14}

The structure and conformation of the Ff filamentous bacteriophages have been characterized by the use of many spectroscopic methods¹⁵ including small-angle X-ray scattering,¹⁶ X-ray

fiber diffraction,^{17–20} Raman,^{21,22} circular dichroism,²³ IR and fluorescence spectroscopy, static solid-state NMR,²⁴ and recently also magic-angle spinning (MAS) NMR.²⁵ At high concentrations, these phages are arranged in hexagonal arrays and may form smectic and cholesteric liquid crystals depending on concentration and ionic strength.²⁶ Every single virion is made of a capsid consisting of pentamers of the major coat protein that are related by an approximate 2-fold screw axis.^{18,27} The rise of successive pentamers is 16.0–16.15 Å depending on the conditions, and the twist between pentamers range between 33° and 36°. The structure of the 50-residue coat protein is of a gently curved right-handed α -helix²⁸ tilted at an angle of ~20° with respect to the viral axis, its positively charged C-terminal residues are buried on the interior of the virus particle where they interact with the DNA,^{15,29} and the N-terminal residues are exposed on the exterior of the particles and undergo motion on the

Received: August 18, 2011**Revised:** November 15, 2011**Published:** November 15, 2011

microsecond time scale.³⁰ Isolated coat proteins reveal a structure of two bent helices in micelles³¹ and in lipid bilayers.³²

Wild-type M13 and fd differ by less than 3% in nucleotide sequence and their coat proteins differ by only a single amino acid; Asn12 in M13 corresponds to Asp12 in fd. At pH 8, the difference is manifested as an additional negative charge in every coat protein in the capsid of the fd phage, which exhibits 10 e⁻/nm whereas for M13 there are 7 e⁻/nm. Structurally, these two phages are most usefully thought of as mutants of each other. It was shown using fiber diffraction data that changes in the helical symmetry of the coat protein in M13 and fd bacteriophage are correlated with changes in the surface charge, and therefore it was suggested that fd and M13 may have a different helical symmetry;³³ however, other studies treat the Ff structures uniformly and the accessibility of Asx12 to the outside of the virion suggested that structural variations should be minor.²⁰ The close environment of the mutant amino acid shows³⁴ that stabilizing salt bridges can form between Lys8 and Asp12, Asp5, and Asp4 in every subunit *j* of fd, as well as linkage to Glu20 of subunit *j* + 6. In M13, similar salt bridges can form, with the exception of residue 12. Mutations between charged and neutral amino acids caused corresponding changes in the electrophoretic mobility of the intact viruses³⁵ and it was observed that the effect of mutations in position 12 is smaller than mutations in position 2.

In order to determine whether the charge and electrophoretic mobility differences between fd and M13 are associated with structural differences, and in order to examine the extent of similarities between the two virions, we applied MAS solid-state NMR to study M13 and fd. The application of the MAS NMR technique, which has developed tremendously in recent years toward the characterization of complex systems such as protein assemblies,^{36–42} membrane proteins,^{43–48} and amyloids,^{49–53} has already proved useful for the study of filamentous bacteriophage viruses, namely, the Pf1 phage^{54–56} and recently also the fd phage.²⁵ In this study, we were able to detect very high similarities between the two phages and, however, also very specific differences in structure and dynamics located mainly at and around the mutation region.

■ EXPERIMENTAL METHODS

Preparation and Characterization of Phage Samples. Experimental data for M13 were obtained using the M13KO7 helper-phage strain bearing kanamycin resistance. Experimental data for fd were obtained using the fth1 strain⁵⁷ bearing tetracycline resistance. The lengths of the genomes are slightly different, 8233 nucleotides (*nt*) for fd and 8669 *nt* for M13. Global sequence alignment of the two circular genomes yields slightly less than 60% identity; however, they have ~97% identity if the tetracycline and kanamycin resistance sections are removed. The wild-type genomes (6407 *nt*) differ by less than 3%.⁵⁸ The fully [¹³C, ¹⁵N]-enriched samples therefore have molecular weights of 22–23 MDa. Both bacteriophages were grown in minimal media on *Escherichia coli* DH5αF' cells following optimized common bacteriological techniques. Explicit details on the production of purified [¹³C, ¹⁵N]-enriched Ff phages were described for fd²⁵ and the preparation of M13 was similar. Sample purity was determined by UV spectrophotometry and infectivity was monitored for all samples. The pure samples (concentration of 1 mg/mL, 10 mM Tris buffer, pH 8.0) were precipitated by adding PEG 8000 to a final concentration of 5%

(w/v) followed by the addition of 5 mM MgCl₂. Pelletings and transfers by centrifugation at 14 000 rpm yielded hydrated fd and M13 samples of ~12 mg virus in pellets of approximately 50 μL in the 4 mm WB zirconium spinning rotors (manufactured by Bruker) for the NMR experiments.

NMR Experiments and Data Analysis. NMR data were collected on a Bruker Avance-III spectrometer operating at a static magnetic field of 14.1 T, corresponding to Larmor frequencies of 600.2 MHz for ¹H, 150.9 MHz for ¹³C, and 60.8 MHz for ¹⁵N. Multidimensional MAS NMR experiments were performed using the Bruker BioSpin's 4 mm E-free probe and a wide-bore 4 mm triple-resonance probe, both operating in ¹H–¹³C–¹⁵N mode. Two-dimensional (2D) ¹³C–¹³C chemical shift correlation spectra were acquired using the modified proton-driven spin-diffusion⁵⁹ sequence DARR⁶⁰/RAD⁶¹ (dipolar-assisted rotational resonance/RF-assisted diffusion), the radio frequency driven recoupling⁶² (RFDR) experiment, and the zero-filtered refocused- (zfr) INADEQUATE experiment.^{63,64} Five data sets were acquired using DARR mixing times of 15, 50, 100, 250, and 500 ms, one data set using RFDR with a mixing time of 3 ms, and the zfr-INADEQUATE experiment with scalar-coupling evolution delays of 3 ms. The three-dimensional (3D) experiments NCACX and NCOCX^{65–67} were acquired using the double cross-polarization scheme⁶⁸ (DCP) followed by DARR/RAD mixing. ¹³C (in 2D) and ¹⁵N (3D) magnetizations were generated using a 10% linearly ramped cross polarization^{69,70} (CP) with the center of the ramp corresponding to the first Hartmann–Hahn spinning sideband⁷⁰ using a radio frequency (RF) power of $\omega_{1H} = -\gamma_{HB_1} = 65$ kHz on protons. During all evolution periods, proton decoupling was applied ($\omega_{1H} \sim 80$ kHz) using mostly the swept-frequency two-pulse phase modulation technique (swf-TPPM⁷¹). ¹³C and ¹⁵N power levels of 50 kHz were used for short pulses and the carrier frequency was centered at 103.6 ppm for all 2D experiments in order to cover the entire spectral width efficiently. Spinning rates were set between 12 and 13.5 kHz. Other experimental parameters can be found in the captions and in the Supporting Information.

The NMR data were processed with the NMRPipe software⁷² and subsequently analyzed using the program Sparky.⁷³ The chemical shift table generated by Sparky reported standard deviations of 0.08 ± 0.04 ppm for the ¹³C shifts across the protein, and 0.12 ± 0.06 for ¹⁵N. Typical line widths (broadened by homonuclear ¹³C–¹³C scalar couplings) were on the order of 70–120 Hz.

■ RESULTS AND DISCUSSION

Resonance Assignment of the Intact M13 Bacteriophage. Site-specific assignment of the ¹³C and ¹⁵N resonances belonging to the major coat protein in intact M13 was obtained by performing a series of dipolar-based 2D and 3D correlation experiments using standard techniques,^{66,74–77} and by collecting data from the J-based MAS-INADEQUATE experiment.⁶⁴

Dipolar-Based Experiments. The spectral region shown in Figure 1a is a portion of the complete Fourier-transformed 2D ¹³C–¹³C homonuclear correlation experiment collected for the intact uniformly labeled M13 phage. The experiment was performed with a mixing time of 100 ms (DARR100) and provided many inter-residue Cα–Cα contacts. The spectrum is governed by the capsid protein (consisting of approximately 87% the total virion mass) and shows the “backbone walk” of residues

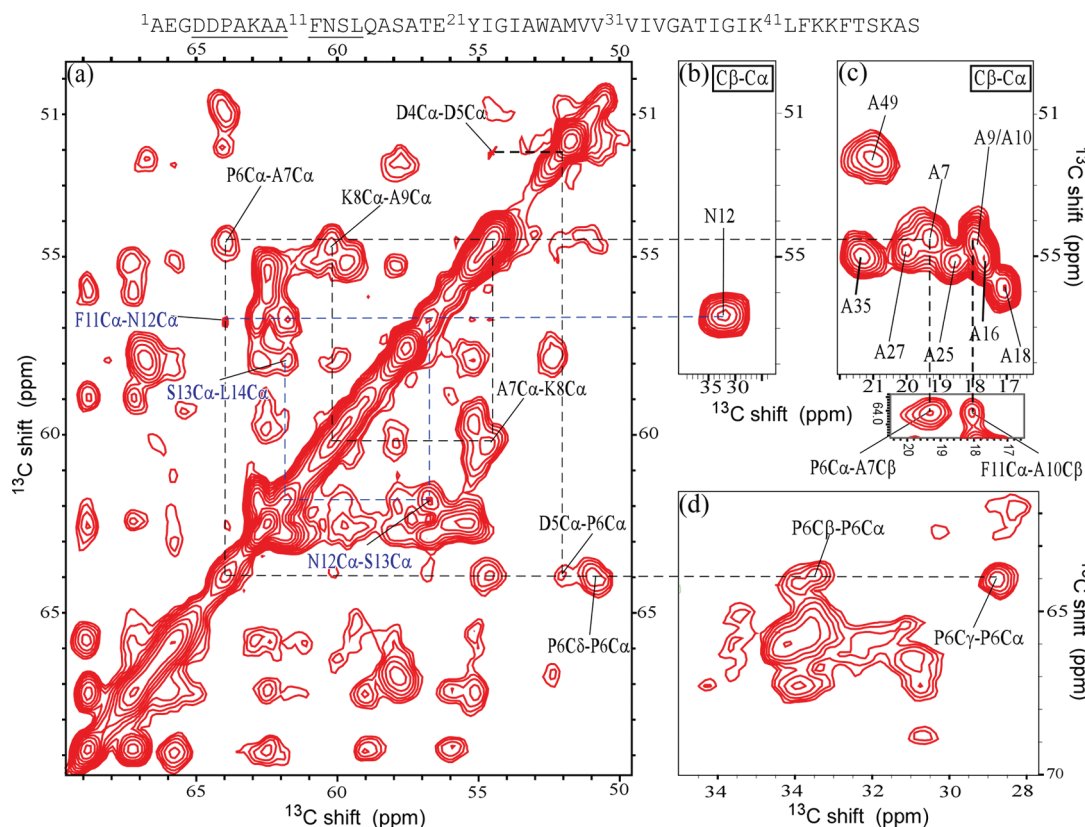


Figure 1. Portions of the 2D ^{13}C – ^{13}C DARR spectra for the intact M13 bacteriophage dominated by contributions from the 50-residue multicopy coat protein (sequence on top). (a) A spectrum acquired at a mixing time of 100 ms: inter-residue $\text{C}\alpha$ – $\text{C}\alpha$ correlations for residues 4–9, 11–14. (b–d) Spectra acquired at a mixing time of 15 ms showing the $\text{C}\alpha$ – $\text{C}\beta$ resonances of (b) Asn12, (c) all alanines, and (d) Pro6. Ala10 was assigned using the correlation of its $\text{C}\beta$ to Phe11 shown in the inset below (c) taken from spectrum (a). All spectra were recorded using a spinning rate of 13.5 kHz and acquisition times of 12.8 and 25 ms in t_1 and t_2 , respectively. Data were acquired for 12 h using a recycle delay of 2.7 s, corresponding to ST_1 (measured by a saturation recovery experiment). A Lorentz-to-Gauss apodization function was used in both dimensions followed by zero filling to $4096(t_1) \times 8192(t_2)$ prior to Fourier transformation. Contour levels are shown from 8σ (σ being the noise root-mean-square determined by SPARKY), with each additional level multiplied by 1.4.

4–14. The assignment of the α -carbons was facilitated by using the known average shifts of amino acids (relying on the entries in the Biological Magnetic Resonance Bank, BMRB⁷⁸), the average shifts of secondary structure elements⁷⁹ and correlations to side-chain carbons. Finally, the data was compared to the assignment of the fd phage.²⁵ Especially important anchoring points were the unique proline resonances (Pro appears only once in the sequence), the isolated Ala $\text{C}\alpha$ – $\text{C}\beta$ shifts, and the distinct difference between Asn12 and Asp12 resonances of the two phages. Cross peaks from Pro6, Phe11, Asn12, and alanines are shown explicitly in Figure 1b–d.

In order to complete the assignment, we performed three-dimensional NCACX and NCOCX experiments. These experiments allowed us to confirm the $\text{C}\alpha$ assignments from the 2D spectra and provided the ^{15}N and $^{13}\text{C}'$ shifts, which were essential for secondary structure calculation and for comparison with the fd phage (strip plots from 3D heteronuclear correlation experiments for residues 12–17 are shown in the Supporting Information). Despite excellent signal to noise, several carbonyl shifts were still missing (mainly at the mobile N-terminus) or highly overlapping. Even for those shifts that were clearly isolated, the 3D NCOCX spectra yielded relatively broad lines due to the short evolution period. In order to remove ambiguities and obtain more accurate and complete assignments, we reverted to J -based spectroscopy.

J-based zfr-INADEQUATE. Adapted from solution NMR,⁸⁰ the INADEQUATE experiment was successfully applied to MAS ssNMR of fully labeled proteins and to organic and inorganic materials.⁶⁴ The use of z-filter refocused (zfr) INADEQUATE in MAS ssNMR proved useful for the removal of many antiphase terms leaving only those emerging from zero-quantum (ZQ) coherences.⁸¹ On isotopically enriched, strongly proton-coupled spin systems, these artifacts cannot be fully removed even when the strong ^1H – ^{13}C dipolar interaction is allowed to dephase the ZQ terms. Therefore, negative and antiphase “long-range” and “relayed” peaks⁸² resulting from multispin contributions complicate the observed spectrum. Nevertheless, we find these peaks extremely useful for the validation and extraction of many resonances belonging to either dynamic residues or to amino acids in congested regions of the 2D single-quantum dipolar-based ^{13}C – ^{13}C spectra of M13.

Figure 2 shows an extracted region from the zfr-INADEQUATE spectrum of the M13 bacteriophage. Expected short-range cross peaks corresponding to one-bond connectivities were identified as sharp intense and mostly in-phase peaks. The one-bond cross peaks were assigned and confirmed the results observed through the dipolar-based experiments. The most substantial contribution of the one-bond INADEQUATE correlations was in obtaining a full pattern for the mobile

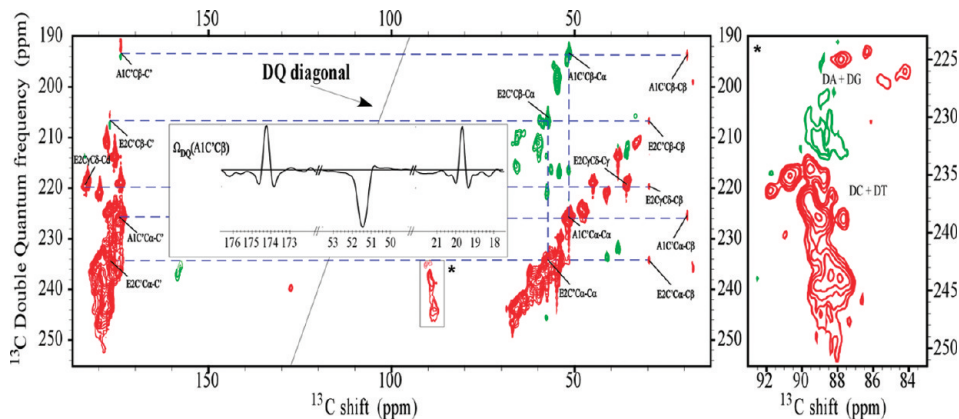


Figure 2. DQ/SQ zero-filtered refocused-INADEQUATE J -based ^{13}C – ^{13}C correlation spectrum of a fully enriched M13 bacteriophage. Positive (red) and negative (green) in-phase cross peaks, and antiphase peaks, are observed in the spectrum. Long-range and relayed correlations of Ala1 and Glu2 are noted in dashed lines. A 1D slice at the double-quantum frequency of 193.5 ppm is shown in the inset and corresponds to the long-range Ala1 C' – $\text{C}\beta$ peak that also exhibits a negative resonance at its $\text{C}\alpha$ shift. The DNA correlation region is marked with an asterisk and its enlargement is depicted on the right. A delay of 3 ms was used during the evolution of scalar couplings. A total experimental time of 77 h was used to collect data corresponding to acquisition times of 5 ms (712 increments) and 20 ms in indirect and acquisition dimensions, respectively. The left spectrum was processed with exponential broadening (50 Hz- t_1 , 100 Hz- t_2) and is plotted using fifteen contour levels starting at 10σ and using a multiplicity of 1.4. The DNA region (right spectrum) was processed with a squared cosine-bell function and contour levels are shown from 6σ , with each additional level multiplied by 1.4. Both spectra were zero filled to 8192 (t_2) \times 4096 (t_1) points prior to Fourier transformation.

N-terminus part of the protein, and in resolving several ambiguities in the dipolar-based experiments (e.g., Thr and Val residues) due to the improved spectral dispersion in the DQ dimension. Especially useful were cross peaks involving carbonyl carbons as their position could now be easily calculated and located unambiguously based on their coupling partner. As an example of the observed coherences, we chose to show the first two residues belonging to the mobile N-terminus of the coat protein. For example, the resonances of Ala1($\Omega_{\text{C}'\text{Ca}}, \omega_{\text{Ca}}$) and Glu2($\Omega_{\text{C}'\text{C}\delta}, \omega_{\text{C}\delta}$) are clearly observed in the spectrum (Ω_{xy} is the sum frequencies of x and y , appearing in the DQ dimension). In addition, relayed cross peaks between nonbonded nuclei sharing a common coupling center were observed as intense negative cross peaks and long-range correlations between nuclei two-bonds apart were also observed, usually as antiphase peaks, similarly to those reported in previous studies.^{81,82} Example for a relayed peak is Glu2($\Omega_{\text{C}'\text{Ca}}, \omega_{\text{C}\beta}$) where the well-resolved $\text{C}\beta$ resonance allowed the new assignment of the Glu2 carbonyl shift. Long-range correlations were also observed in the spectrum (Ala1 C' – $\text{C}\beta$, Glu2 C' – $\text{C}\beta$) and despite their weak intensity and antiphase nature they could be unambiguously assigned due to the intermediate connecting spins (Ala1– $\text{C}\alpha$, Glu2– $\text{C}\alpha$). Important to note is that for the two amino acids shown in Figure 2a the C' atoms were undetected in the dipolar-based experiments and unassigned in fd. The relayed and long-range correlations in the INADEQUATE spectrum facilitated the assignment of many C' atoms by a simple calculation of their position despite the spectral congestion in that region.

Additional correlations belonging to the DNA of M13 were also detected in the INADEQUATE spectrum (the expansion of the region denoted by an asterisk is shown in Figure 2). Long-range 2J couplings revealed resonances corresponding to the deoxyribose $\text{C}1'$ carbons (84–90 ppm) and their attached bases, C2 and C6 in cytosine (dC) and thymine (dT), C4 and C8 in adenine (dA) and guanine (dG). Additional resonances belonging to correlations of other deoxyribose carbons with $\text{C}1'$ were also observed in our spectrum (not shown). Based on average

chemical shifts in the BMRB and on the table of base- ^{13}C shifts in B-DNA provided by Sergeyev et al.,⁸³ we could qualitatively separate the contributions of dC and dT from those of dA and dG. A few weak cross peaks ($\Omega_{\text{C}4/\text{C}1'}, \omega_{\text{C}1'}$) belonging to dA and dG appear at DQ frequencies of 225–235 ppm (upper-right part of the spectrum). Much stronger correlations are observed for dC and dT. Their $\text{C}1'$ resonances appear between 87.5 and 90 ppm and at DQ frequencies spanning 230–245 ppm and are consistent with reported average values of the attached base carbons (dC–C2 \sim 159.5, dC–C6 \sim 142.9, dT–C2 \sim 151.6, dT–C6 \sim 138.2). Although currently only limited information could be obtained on the DNA base chemical shifts, clearly the use of scalar couplings for magnetization transfer and the dispersion along the DQ dimension will allow a better qualitative assessment of DNA conformation in filamentous bacteriophage due to the accumulating knowledge on the relation between DNA shifts and conformation.

Comparison of fd and M13. Once assignment of the M13 phage has been completed, comparison of the spectral data of fd and M13 provided further insight into their differences and similarities. Figure 3a shows an overlay of M13 and fd spectra cut at the carbonyl (bottom), $\text{C}\alpha$ side chain (middle), and glycine (top) regions of a ^{13}C – ^{13}C correlation spectrum. Similarly to fd, signals from M13 show excellent resolution. It is immediately apparent that the β -carbons of Asp12 and Asn12 are different (38.3 and 40.2 ppm, respectively) and their identity can be easily verified by virtue of their correlation to the α -carbons (56.7 and 57.7 ppm, respectively) and to additional neighboring amino acids (e.g., middle spectrum, correlation to Ser13). However, the majority of the spectral features indicate extensive similarity; resonances at the $\text{C}\alpha$ side-chain region, which exhibit peak positions that are a good measure of the backbone torsion angles, are identical (aside from Asx12); medium range contacts of all glycines are identical (top); and the side-chain region shows mostly identical peaks for the two phages (Figure 4, marked in black). The fact that all Ile, Leu and Val side chains show identical shifts suggests similar subunit packing in the hydrophobic

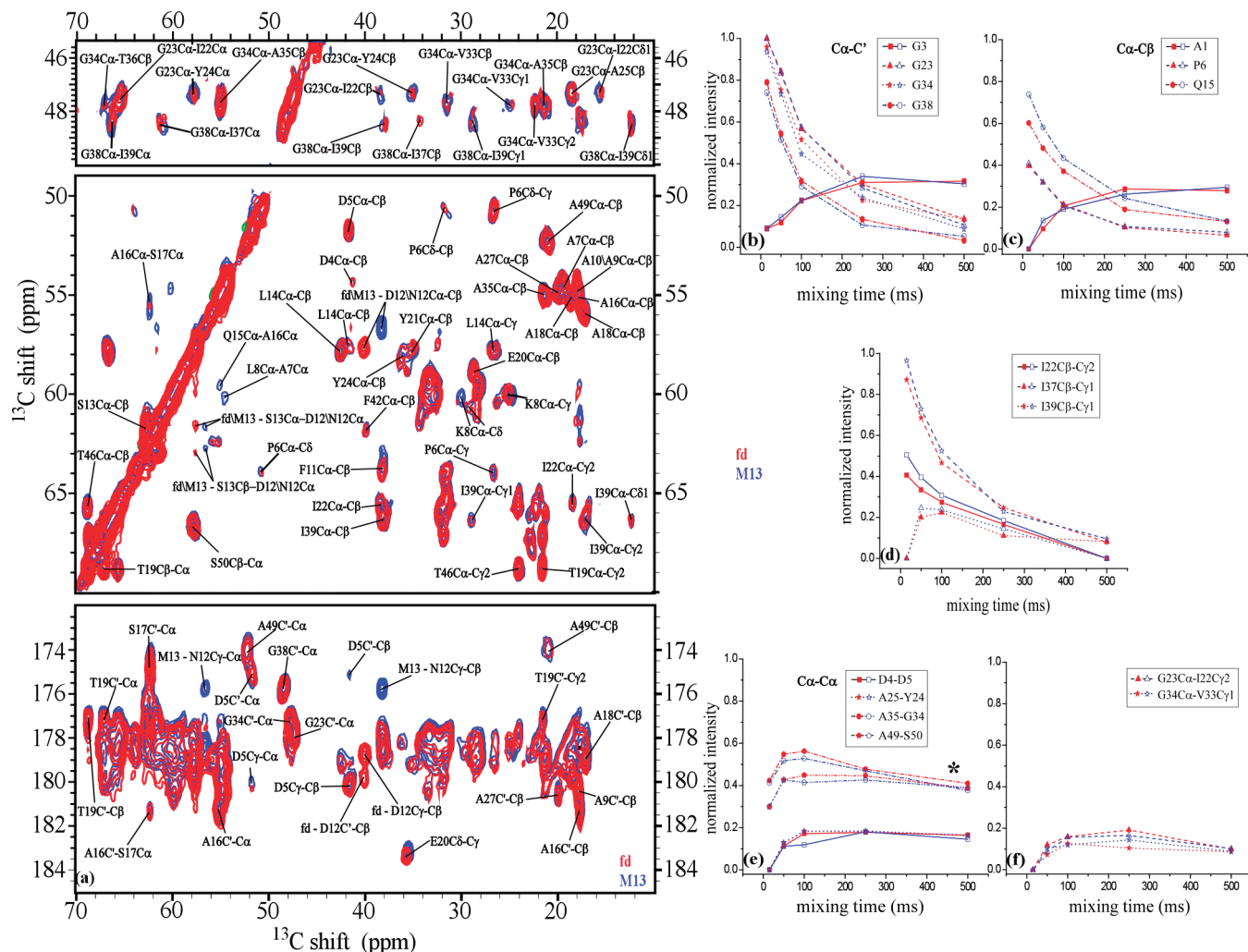


Figure 3. Similarities in structure and dynamics between M13 and fd bacteriophages. (a) Extracted regions from 2D ^{13}C - ^{13}C DARR spectra of intact M13 (blue) and fd (red) bacteriophages. Mixing times were 100 ms for the top spectra and 15 ms for the middle and bottom spectra. (b–f) Normalized intensities (calibrated to the signals of $\text{G}23\text{Ca}-\text{C}'$ at a mixing time of 15 ms) of cross peaks from different mixing times; (b) glycine $\text{Ca}-\text{C}'$ correlations; (c) single-bond correlations of A1, P6, and Q15; (d) Ile side-chain correlations; (e) backbone inter-residue correlations; (f) inter-residue correlations of glycine backbone α -carbons and neighboring amino acid side chains. The normalized intensities for two build-up curves (A35C α -G34C α and A49C α -S50C α) in (e) were elevated by 0.3 for clarity (marked with asterisk). Acquisition and processing parameters are as in Figure 1.

regions along the capsid.⁵⁵ In addition, lysine side chain atoms belonging to the DNA interaction region, despite their significant spectral overlap, show identical shifts as well (not shown). A calculation of the differences between the chemical shifts of M13 and fd for the entire sequence, removing the unique residues that produce shift deviations, gives $\Delta\text{C}\alpha=|\text{C}\alpha(\text{M13})-\text{C}\alpha(\text{fd})|=0.07 \pm 0.06$ ppm, $\Delta\text{C}\beta=0.08 \pm 0.07$ ppm, and for all other side chain carbons $\Delta\text{C}=0.07 \pm 0.06$. These numbers are similar or even smaller than average errors reported for many other globular proteins (according to solid state NMR BMRB entries) and must indicate a very robust structure for the virion capsids, which is maintained despite their different lengths and DNA constructs. Our data is also consistent with the observation of subunit structure similarity by other spectroscopic methods, and is an implication of the biological stability of these phages. The only apparent significant differences are observed for the side chain of Lys8 and for a few other atoms, as will be discussed below.

Another strong marker indicating the similarities between the two virions comes from analysis of the cross-peak intensities at different mixing times. Since molecular motions on the microsecond–millisecond time scale average the dipolar couplings hence affecting the intensity of the build-up curves, similarity of the cross-peak intensities in both phages must indicate highly similar flexibility. We have analyzed the build-up curves of many one-bond and longer-range ^{13}C pairs that rise from well-isolated peaks in our 2D data and some of the results are indicated in Figure 3b–f. In order to account for the different signal to noise and quantities of M13 and fd samples, we normalized peak intensities to that of the single-bond cross peak Gly23C α -C β . The build-up curve similarities were reproducible for several samples. In Figure 3b, the cross peaks of GlyC α -C β reveal almost indistinguishable intensities. Similar trends are observed for the three representative single-bond C α -C β cross peaks in (c) (residues Ala1, Pro6, Gln15 in Figure 3c). Even for Ile side chains that may be more flexible and susceptible to changes due

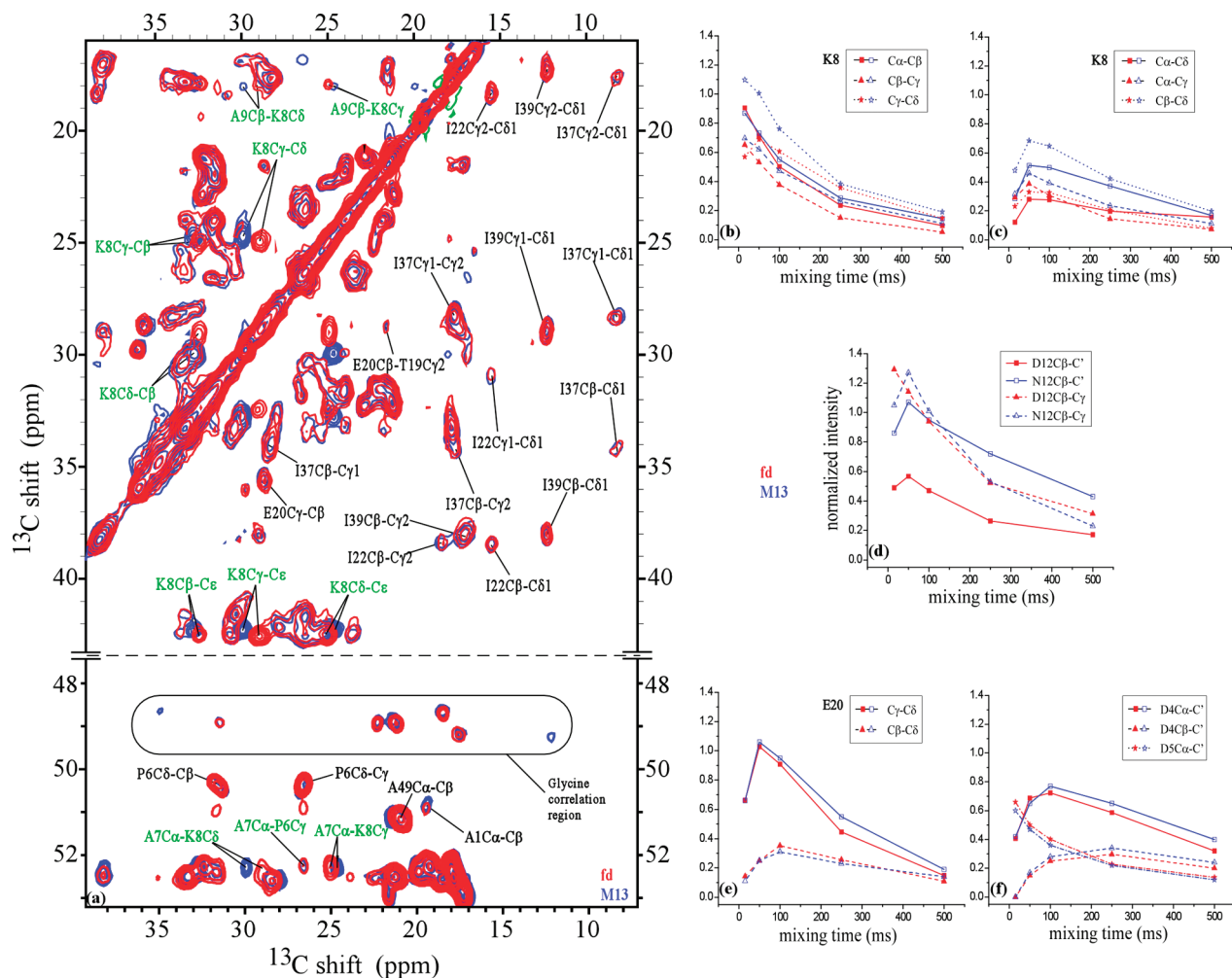


Figure 4. Differences in structure and dynamics between M13 and fd bacteriophages. (a) Aliphatic side-chain region cut from 2D ^{13}C – ^{13}C DARR100 spectra of intact M13 (blue) and fd (red) bacteriophages. The lower spectrum (below the dashed line) was obtained from a different, concentrated fd sample, and exhibits improved signal to noise allowing to compare the glycine correlation region and the inter-residue correlations; (b–f) cross-peak intensities for fd and M13 normalized separately to the Gly23C α –C' shift (at a mixing time of 15 ms); (b,c) intensities associated with Lys8; (d) intensities associated with Asx12; (e,f) intensities associated with other charged residues in the same region showing similar dynamics properties.

to sample preparation, cross-peak signals are nearly identical (Figure 3d) and analysis of longer-range inter-residue cross peaks (Figure 3e–f) show complete identity between fd and M13. These high similarities in chemical shifts and cross-peak intensities must reflect a true physical stability and robustness of every single filamentous phage structure, which provides them with the ability to survive in various host environments under variable pH and salinity conditions. We reassured our results by analyzing curves corresponding to peaks across the diagonal; despite the fact that their absolute intensity differed, here also fd and M13 perfectly overlaid. The asymmetry is a result of uneven initial excitation of the various carbon spins, the number of neighboring spins for each carbon (e.g., C γ –C β is expected to be different from C β –C γ since C β transfers polarization also to C α as a second nearest neighbor) and also a result of the uneven magnetization transfer when a sideband of one spin partially overlaps with the center band of the other.⁸⁴

Apart from the similarities of almost all resonances in the spectrum (for the assigned and very few unassigned peaks) and the obvious differences in Asx12 resonances, there are significant differences (≥ 0.3 ppm, see Table 1) for the Lys8 side-chain

carbon resonances ($\Delta\delta = 0.3$ –0.9 ppm) and for several more shifts in the same region including Gln15–C β and Gln15–C γ ($\Delta\delta = 0.3$ ppm) and Tyr24–C γ ($\Delta\delta = 0.4$ ppm, see Supporting Information for the spectrum). Such differences are significantly larger than the average $\Delta\delta \sim 0.1$ indicated previously, and probably reflect some rearrangement of side-chain interactions within a single subunit or also between subunits. The most significant shift deviations of Lys8 are shown in the ^{13}C correlation spectrum in Figure 4, where resonances from its entire side chain are indicated, and can easily be identified via their mutual cross peaks, and via inter-residue cross peaks.

Additional notable differences (excluding $\Delta\delta_{15\text{N}}$ of Asx12 of 2.7 ppm) in this region are for the ^{15}N shifts of Ala10 (2 ppm), Phe11 (2.2 ppm), and Ser13 (0.5 ppm). Since ^{15}N shifts are especially sensitive to hydrogen-bonding patterns, nearest-neighbor effects, and the first side-chain torsion angle χ_1 , it is not surprising that the modification of the amino acid and the structural change in residue 8 are manifested as large ^{15}N shift perturbations in almost all residues in that region. This suggests a local structural change between M13 and fd in the intersubunit packing and electrostatic interactions driven by the Lys8 amino

acid. However, changes in this region are not restricted to chemical shifts alone. Analysis of magnetization build-up curves for Lys8 of both phages (Figure 4b,c) shows increased differences in the dynamic properties of atoms along the chain. In particular, the intensities associated with M13 of both Asx12 and Lys8 suggest increased rigidity or more restriction in motion over fd. Interestingly, the negatively charged residues (Glu20, Asp4, Asp5 in Figure 4e,f) do not exhibit such variations. Analysis of the corresponding symmetric cross peaks across the diagonal shows small variations in the intensities for fd that mainly supports our assumption for the increased rigidity of the M13–Lys8 amino acid (data not shown).

Table 1. Chemical Shift Differences of the Residues in the Vicinity of Asx12 (Absolute Values in ppm)^a

	$\Delta C'$	$\Delta C\alpha$	$\Delta C\beta$	$\Delta C\gamma$	$\Delta C\delta$	$\Delta C\epsilon$	ΔN
D4	0.0	0.0	0.1	na	—	—	na
D5	0.1	0.1	0.1	0.1	—	—	0.1
P6	0.1	0.0	0.1	0.1	0.0	—	na
A7	0.2	0.0	0.1	—	—	—	0.2
K8	0.6	0.1	0.3	0.3	0.9	0.3	0.1
A9	0.1	0.1	0.0	—	—	—	0.3
A10	2.2	0.0	0.1	—	—	—	2
F11	0.1	0.2	0.1	0.6	na	na	2.2
D12/N12	1.3	1.1	1.9	2.9	—	—	2.7
S13	0.1	0.0	0.2	—	—	—	0.5
L14	0.1	0.0	0.1	0.0	0.0	—	0.3
Q15	0.1	0.1	0.3	(0.3)	na	—	0.3

^a Unassigned resonances are marked “na”. Significant differences ($\Delta C \geq 0.3$ ppm, $\Delta N \geq 0.4$ ppm) are emphasized in boldface. The Gln15–C γ resonance exhibits overlap and the data is ambiguous.

A comparison of several entries^{20,24,85,86} for fd-Y21M (fd bearing a Tyr21 to Met mutant in the coat protein) in the Protein Data Bank reveals that Lys8 is in close proximity to Asp5 and Asp12 within the same subunit, and to Glu20 of a different subunit (related by a single translation along z of 16.15 Å and rotation of 36° according to the 2C0X entry⁸⁵). In addition, it may interact via a hydrogen bond with Tyr21 and Tyr24 of a different subunit. In order to demonstrate the electrostatic interactions and hydrogen-bonding patterns surrounding Lys8 (Figure 5), we chose the structure from PDB entry 2C0X, which was refined against both X-ray and NMR data using simulated annealing (energy minimization was performed in Cartesian coordinates allowing flexibility of the planar angle ω). Distances between the amidic nitrogen of Lys8 and the oxygen atom of the negatively charged carboxylic group in this structure and in others (not shown here) range from 5.8 to 6.4 Å to Asp4, 4.9–5.2 Å to Asp5, and 1.9–4.5 Å to Glu20, with a much larger distance of 7.8 Å in the model from CryoEM.⁸⁶ The distances proposed for Lys8–Asp12 in fd range from 6.6 to 7.3 Å (the different PDB models we used, 1IFJ, 1IFD, 2C0W, 2C0X, 2HIS, and 1NH4 were aligned using the backbone atoms of residues 4–12, and subunits j + 6 and j + 11 were generated using the reported phage symmetry of each entry). In M13, Asn12 replaces Asp12 and one negative charge is eliminated. As suggested above, this can cause the lysine side chain to shift toward the aspartate residues in positions 4 and 5 creating a tighter and more rigid salt bridge than in fd. If this hypothesis is correct, then in fd the lysine side chain may exhibit more dynamics, shifting between the negative charge of Asp4/S on one side and Asp12 on its other side, as manifested in the build-up curves in Figure 4. Such effects must influence at least in part the aromatic amino acids and indeed we see a significant shift (0.4 ppm) for the C γ of Tyr24. Due to spectral overlap, broadening by scalar couplings, and reduced signal to

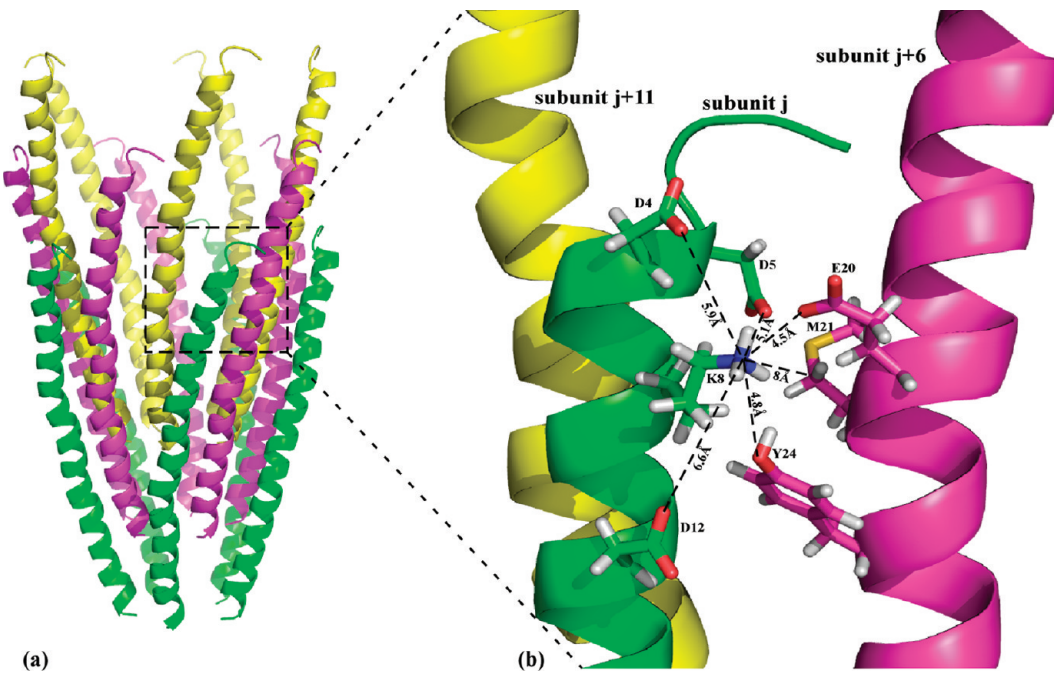


Figure 5. (a) Fifteen subunits (3 pentamers) of the fd-Y21M bacteriophage major coat protein. Each pentamer is colored differently; (b) view from the outside of the fd virion on the K8 interaction pocket. Major coat protein subunit j (green), j + 6 (magenta), and j + 11 (yellow) along with the possible intra- and intersubunit contacts are shown. Side-chain atoms for D4, D5, K8, and D12 in subunit j and E20, M21 (Y21 in wt) and Y24 in subunit j + 6 are shown in a stick model. The structure was generated by the program PyMOL using the coordinates of the entry 2C0X.

noise, it is hard to unambiguously determine if other ring carbons are significantly shifted as well.

Many studies have revealed charge-related differences between fd and M13. From titrations we learn⁸⁷ that the only charges that are exposed to solvent electrolytes (above the isoelectric point of 4.2) are those on the N-terminal part of the protein, i.e., the amino terminal group of Ala1, the negative charges of Glu2, Asp4, Asp5, Asp12, and Glu20, and the positive charge on Lys8. Other charges in the C-terminus are compensated for by the DNA phosphate head groups and become exposed only at very low pH values. The different surface charges were shown to affect several global structural changes: a shift in the isotropic–cholesteric liquid crystal phase transition^{11,88} results from the change in effective diameter of M13 and fd (which is influenced by surface charges and the ionic strength of the solution). Also, in a comparative study of several Ff mutants at pH 2 and 8, Makowski et al. suggested³³ that the surface charge affects the symmetry of the virions; at pH 2 all strains studied (M13, fd, fd-Y24F) are positively charged (where the total charge is approximately +2) and exhibit a C₅S₂ symmetry. At pH 8, fd and fd-Y24F have a more negative charge than M13 and show small but somewhat different deviations from the exact twofold screw axis symmetry. It was therefore deduced that the charge has a significant effect in stabilizing the symmetry, but it is not the only factor. As pointed out by Marvin et al.,²⁰ replacement of the charge can produce local changes, and while in fd Asp12 may form a salt bridge with Lys8, in M13 Asn12 is likely to form hydrogen bonds with Y24 of a neighboring subunit. Our data support this assumption since we observe both chemical shift deviations in the side chain of Y24 and different dynamic behavior of the Asx12 residues in M13 and fd. The different charges in fd and M13 were also shown to affect the electrophoretic mobility of the two phages.^{11,35} Interestingly, mutants in which the negative charge was removed from residue 2 (E2L/Y/S) and have two Asp residues at positions 5 and 12 move faster (relative mobility of 0.88) than mutants that have the D12N modification (0.81)³⁵ and a similar total charge. This result is in line with our proposition that the side chain of Lys8 may change its conformation in M13, or experience a different electronic environment and thus may form a tight salt bridge with Asp5 thereby being screened and reducing the mobility; on the other hand, when the two negative charges are on Asp5 and 12 (as for fd), the positive charge on Lys8 is not efficiently screening the negative charges and the mobility may partially increase.

Interestingly, aside from the variations in Lys8 in the C-terminus part of the protein, another difference we observe is the appearance of an additional pattern of cross peaks that exist only in the M13 spectra (within the signal to noise of our experiments). Correlated resonances appear at chemical shifts of 16.8, 17.9, 26.6, and 34.7 ppm (see Supporting Information). Such a chemical shift pattern can match an Ile side chain and may belong to Ile32, although no linkage to neighboring amino acids could be established. We have shown previously that for fd the side-chain resonances belonging to Ile32 spread over a range of more than 1 ppm, suggesting the existence of some local polymorphism (with values around 38, 29.8, 16.9, and 13.7 ppm for carbons β , γ_1 , γ_2 , δ_1 , respectively). We observed similar results for M13, and these resonances (in both virions) could clearly be site-specifically assigned by the detection of inter-residue cross peaks. Observation of Ile32 in a model from PDB entry 2C0X using 15 subunits reveals that the long side chain of Ile32 is pointing inward, in close proximity to the DNA. Alignment of the DNA sequences of

the two phages shows that identical regions are located in different parts of the DNA and that some variations in length and identity of nucleotides exist. It is possible that for M13 other conformations of Ile32 exist that interact with different parts of the DNA; however, we have no other evidence for this assumption and such variations are not observed for the C-terminal lysine resonances, which are presumably in contact with the DNA phosphate headgroups.

■ SUMMARY AND CONCLUSIONS

The M13 bacteriophage has been studied by magic-angle-spinning solid-state NMR and compared to the closely related fd phage. Aside from the use of 2D and 3D dipolar-based correlation experiments for the assignment of the M13 coat protein, we show here the contribution of the through-bond J-based zfr-INADEQUATE experiment and in particular the advantage of exploiting relayed and long-range peaks observed in this experiment. In addition, resonances emerging from deoxyribose carbons and ²J scalar couplings between sugars and bases in the DNA have been observed and qualitatively assigned. From comparison of chemical shift resonances and cross-peak buildup curves in dipolar-based homonuclear correlation experiments, we deduce that the structures of the two phages are very similar but several local differences do exist. Careful examination of the different spectra reveal that over the entire capsid assembly average chemical shift deviations are in the order of 0.1 ppm, a value that is smaller or in the order of regular experimental errors encountered for globular proteins. Also, mostly no differences can be observed in the local motion on the time scale of the dipolar interaction despite the different lengths, genome variations, and preparations of the two Ff phages. These observations lead us to believe that the capsid structure is well conserved and suited to withstand the harsh conditions required for the survival of the viruses. On the other hand, differences are observed in the region of residue 12, where the negatively charged residue Asp in fd is replaced with Asn in M13. In addition to studies that showed the effect of the eliminated charge on electrophoretic mobility, global symmetry, and liquid crystalline behavior, we find differences in the structure and dynamics of the positively charged Lys8 residue and a few additional nuclei in its surroundings. The NMR data suggests that this residue adopts a different conformation and is more rigid in M13, probably in order to minimize the energy associated with the new electrostatic and hydrogen-bonding environment in and between subunits. As this small perturbation is repeated thousands of times throughout the entire virion, it is likely to play a significant role in the macroscopic behavior of Ff filamentous phage structure in terms of symmetry and liquid crystal formation. These findings demonstrate that MAS NMR is capable of detecting very small atomic-scale differences in large protein assemblies and in the case of filamentous phage may provide insight into the morphogenesis of apparently similar filamentous viruses.

■ ASSOCIATED CONTENT

S Supporting Information. Experimental and processing parameters, strip plots from 3D spectra demonstrating the assignment of residues 12–17, a list of chemical shift assignment for M13 and deviations between fd and M13, spectral overlay of M13 and fd in additional regions, and full author list for refs 36 and 78. This material is available free of charge via the Internet at <http://pubs.acs.org>.

■ ACKNOWLEDGMENT

Financial support was provided by the Israel Science Foundation (Grant no. 241/08) and the Marie-Curie reintegration grant (EU-FP7-IRG no. 224800). Support for the spectrometer was given by the center for Nanoscience and Nanotechnology of Tel Aviv University. The fth1 vector is a kind gift from Prof. Jonathan Gershoni from the Department of Cell Research and Immunology, Faculty of Life Sciences, Tel Aviv University. The M13K07 phage and the DH5αF' cells are a kind gift from Prof. Itai Benhar, Department of Microbiology and Biotechnology, Tel Aviv University.

■ REFERENCES

- (1) Day, L. A. In *Encyclopedia of Virology*, 3rd ed.; Mahy, B. W. J., van Regenmortel, M. H. V., Eds.; Elsevier: Oxford, UK, 2008; pp 117–124.
- (2) Kehoe, J. W.; Kay, B. K. *Chem. Rev.* **2005**, *105*, 4056–4072.
- (3) Smith, G. P. *Science* **1985**, *228*, 1315–1317.
- (4) Messing, J. *Methods Mol. Biol.* **2001**, *167*, 13–31.
- (5) Sanger, F.; Coulson, A. R.; Barrell, B. G.; Smith, A. J. H.; Roe, B. A. *J. Mol. Biol.* **1980**, *143*, 161–178.
- (6) Merzlyak, A.; Lee, S. W. *Curr. Opin. Chem. Biol.* **2006**, *10*, 246–252.
- (7) Nam, K. T.; Wartena, R.; Yoo, P. J.; Liau, F. W.; Lee, Y. J.; Chiang, Y. M.; Hammond, P. T.; Belcher, A. M. *Proc. Natl. Acad. Sci. U.S.A.* **2008**, *105*, 17227–17231.
- (8) Khalil, A. S.; Ferrer, J. M.; Brau, R. R.; Kottmann, S. T.; Noren, C. J.; Lang, M. J.; Belcher, A. M. *Proc. Natl. Acad. Sci. U.S.A.* **2007**, *104*, 4892–4897.
- (9) Nam, K. T.; Kim, D. W.; Yoo, P. J.; Chiang, C. Y.; Meethong, N.; Hammond, P. T.; Chiang, Y. M.; Belcher, A. M. *Science* **2006**, *312*, 885–888.
- (10) Lee, Y. J.; Yi, H.; Kim, W. J.; Kang, K.; Yun, D. S.; Strano, M. S.; Ceder, G.; Belcher, A. M. *Science* **2009**, *324*, 1051–1055.
- (11) Purdy, K. R.; Fraden, S. *Phys. Rev. E* **2004**, *70*, 061703.
- (12) Grelet, E.; Fraden, S. *Phys. Rev. Lett.* **2003**, *90*, 198302.
- (13) Tombolato, F.; Ferrarini, A.; Grelet, E. *Phys. Rev. Lett.* **2006**, *96*, 258302.
- (14) Barry, E.; Beller, D.; Dogic, Z. *Soft Matter* **2009**, *5*, 2563–2570.
- (15) Day, L. A.; Marzec, C. J.; Reisberg, S. A.; Casadevall, A. *Annu. Rev. Biophys. Biomol. Chem.* **1988**, *17*, 509–539.
- (16) Grelet, E. *Phys. Rev. Lett.* **2008**, *100*, 168301.
- (17) Glucksman, M. J.; Bhattacharjee, S.; Makowski, L. *J. Mol. Biol.* **1992**, *226*, 455–470.
- (18) Banner, D. W.; Nave, C.; Marvin, D. A. *Nature* **1981**, *289*, 814–816.
- (19) Marvin, D. A. *Int. J. Biol. Macromol.* **1990**, *12*, 335–335.
- (20) Marvin, D. A.; Hale, R. D.; Nave, C.; Citterich, M. H. *J. Mol. Biol.* **1994**, *235*, 260–286.
- (21) Williams, R. W.; Dunker, A. K.; Petricolas, W. L. *Biochim. Biophys. Acta* **1984**, *791*, 131–144.
- (22) Thomas, G. J.; Prescott, B.; Day, L. A. *J. Mol. Biol.* **1983**, *165*, 321–356.
- (23) Clack, B. A.; Gray, D. M. *Biopolymers* **1989**, *28*, 1861–1873.
- (24) Zeri, A. C.; Mesleh, M. F.; Nevzorov, A. A.; Opella, S. J. *Proc. Natl. Acad. Sci. U.S.A.* **2003**, *100*, 6458–6463.
- (25) Abramov, G.; Morag, O.; Goldbourt, A. *J. Phys. Chem. B* **2011**, *115*, 9671–9680.
- (26) Dogic, Z.; Fraden, S. *Phys. Rev. Lett.* **1997**, *78*, 2417.
- (27) Caspar, D. L. D.; Makowski, L. *J. Mol. Biol.* **1981**, *145*, 611–617.
- (28) Day, L. A. *J. Mol. Biol.* **1969**, *39*, 265–277.
- (29) Marvin, D. A.; Wachtel, E. J. *Nature* **1975**, *253*, 19–23.
- (30) Colnago, L. A.; Valentine, K. G.; Opella, S. J. *Biochemistry* **1987**, *26*, 847–854.
- (31) Almeida, F. C. L.; Opella, S. J. *J. Mol. Biol.* **1997**, *270*, 481–495.
- (32) Marassi, F. M.; Opella, S. J. *Protein Sci.* **2003**, *12*, 403–411.
- (33) Bhattacharjee, S.; Glucksman, M. J.; Makowski, L. *Biophys. J.* **1992**, *61*, 725–735.
- (34) Scholtz, J. M.; Baldwin, R. L. *Annu. Rev. Biophys. Biomol. Struct.* **1992**, *21*, 95–118.
- (35) Boeke, J. D.; Russel, M.; Model, P. *J. Mol. Biol.* **1980**, *144*, 103–116.
- (36) Poyraz, O.; Schmidt, H.; Seidel, K.; Delissen, F.; Ader, C.; Tenenboim, H.; Goosmann, C.; Laube, B.; Thunemann, A. F.; Zychlinsky, A.; et al. *Nat. Struct. Mol. Biol.* **2010**, *17*, 788–792.
- (37) Han, Y.; Ahn, J.; Concel, J.; Byeon, I.-J. L.; Gronenborn, A. M.; Yang, J.; Polenova, T. *J. Am. Chem. Soc.* **2010**, *132*, 1976–1987.
- (38) Loquet, A.; Lv, G.; Giller, K.; Becker, S.; Lange, A. *J. Am. Chem. Soc.* **2011**, *133*, 4722–4725.
- (39) Siemer, A. B.; Ritter, C.; Steinmetz, M. O.; Ernst, M.; Riek, R.; Meier, B. H. *J. Biomol. NMR* **2006**, *34*, 75–87.
- (40) Chimon, S.; Shaibat, M. A.; Jones, C. R.; Calero, D. C.; Aizezi, B.; Ishii, Y. *Nat. Struct. Mol. Biol.* **2007**, *14*, 1157–1164.
- (41) Mainz, A.; Jehle, S.; van Rossum, B. J.; Oschkinat, H.; Reif, B. J. *Am. Chem. Soc.* **2009**, *131*, 15968–15969.
- (42) Jehle, S.; Rajagopal, P.; Bardiaux, B.; Markovic, S.; Kuhne, R.; Stout, J. R.; Higman, V. A.; Klevit, R. E.; van Rossum, B.-J.; Oschkinat, H. *Nat. Struct. Mol. Biol.* **2010**, *17*, 1037–1042.
- (43) Ahmed, M. A. M.; Bamm, V. V.; Harauz, G.; Ladizhansky, V. *Biophys. J.* **2010**, *99*, 1247–1255.
- (44) Hu, F. H.; Luo, W. B.; Cady, S. D.; Hong, M. *BBA-Biomembranes* **2011**, *1808*, 415–423.
- (45) Shi, L. C.; Kawamura, I.; Jung, K. H.; Brown, L. S.; Ladizhansky, V. *Angew. Chem., Int. Ed.* **2011**, *50*, 1302–1305.
- (46) Su, Y. C.; DeGrado, W. F.; Hong, M. *J. Am. Chem. Soc.* **2010**, *132*, 9197–9205.
- (47) Qiang, W.; Sun, Y.; Weliky, D. P. *Proc. Natl. Acad. Sci. U.S.A.* **2009**, *106*, 15314–15319.
- (48) Yang, J.; Aslimovska, L.; Glaubitz, C. *J. Am. Chem. Soc.* **2011**, *133*, 4874–4881.
- (49) Heise, H.; Celej, M. S.; Becker, S.; Riede, D.; Pelah, A.; Kumar, A.; Jovin, T. M.; Baldus, M. *J. Mol. Biol.* **2008**, *380*, 444–450.
- (50) Helmus, J. J.; Surewicz, K.; Surewicz, W. K.; Jaroniec, C. P. *J. Am. Chem. Soc.* **2010**, *132*, 2393–2403.
- (51) Tycko, R. *Q. Rev. Biophys.* **2006**, *39*, 1–55.
- (52) Jaroniec, C. P.; MacPhee, C. E.; Astrof, N. S.; Dobson, C. M.; Griffin, R. G. *Proc. Natl. Acad. Sci. U.S.A.* **2002**, *99*, 16748–16753.
- (53) Heise, H. *ChemBioChem* **2008**, *9*, 179–189.
- (54) Goldbourt, A.; Gross, B. J.; Day, L. A.; McDermott, A. E. *J. Am. Chem. Soc.* **2007**, *129*, 2338–2344.
- (55) Goldbourt, A.; Day, L. A.; McDermott, A. E. *J. Biol. Chem.* **2010**, *285*, 37051–37059.
- (56) Lorieau, J. L.; Day, L. A.; McDermott, A. E. *Proc. Natl. Acad. Sci. U.S.A.* **2008**, *105*, 10366–10371.
- (57) Enshell-Seijfers, D.; Smelyanski, L.; Gershoni, J. M. *Nucleic Acids Res.* **2001**, *29*, e50.
- (58) van Wezenbeek, P. M. G. F.; Hulsebos, T. J. M.; Schoenmakers, J. G. G. *Gene* **1980**, *11*, 129–148.
- (59) Szeverenyi, N. M.; Sullivan, M. J.; Maciel, G. E. *J. Magn. Reson.* **1982**, *47*, 462–475.
- (60) Takegoshi, K.; Nakamura, S.; Terao, T. *Chem. Phys. Lett.* **2001**, *344*, 631–637.
- (61) Morcombe, C. R.; Gaponenko, V.; Byrd, R. A.; Zilm, K. W. *J. Am. Chem. Soc.* **2004**, *126*, 7196–7197.
- (62) Bennett, A. E.; Griffin, R. G.; Ok, J. H.; Vega, S. *J. Chem. Phys.* **1992**, *96*, 8624–8627.
- (63) Lesage, A.; Bardet, M.; Emsley, L. *J. Am. Chem. Soc.* **1999**, *121*, 10987–10993.
- (64) Lesage, A.; Auger, C.; Caldarelli, S.; Emsley, L. *J. Am. Chem. Soc.* **1997**, *119*, 7867–7868.
- (65) Sperling, L. J.; Berthold, D. A.; Sasser, T. L.; Jeisy-Scott, V.; Rienstra, C. M. *J. Mol. Biol.* **2010**, *399*, 268–282.
- (66) Straus, S. K.; Bremi, T.; Ernst, R. R. *J. Biomol. NMR* **1998**, *12*, 39–50.

- (67) Zhong, L.; Bamm, V. V.; Ahmed, M. A. M.; Harauz, G.; Ladizhansky, V. *BBA-Biomembranes* **2007**, *1768*, 3193–3205.
- (68) Schaefer, J.; McKay, R. A.; Stejskal, E. O. *J. Magn. Reson.* **1979**, *34*, 443.
- (69) Metz, G.; Wu, X. L.; Smith, S. O. *J. Magn. Reson., Ser A* **1994**, *110*, 219–227.
- (70) Stejskal, E. O.; Schaefer, J.; Waugh, J. S. *J. Magn. Reson.* **1977**, *28*, 105–112.
- (71) Vinod Chandran, C.; Madhu, P. K.; Kurur, N. D.; Brauniger, T. *Magn. Reson. Chem.* **2008**, *46*, 943–7.
- (72) Delaglio, F.; Grzesiek, S.; Vuister, G. W.; Zhu, G.; Pfeifer, J.; Bax, A. *J. Biomol. NMR* **1995**, *6*, 277–293.
- (73) Goddard, T. D.; Kneller, D. G. In SPARKY 3.110; University of California: San Francisco, CA, 2004.
- (74) Huang, L.; McDermott, A. E. *BBA-Bioenergetics* **2008**, *1777*, 1098–1108.
- (75) Pauli, J.; Baldus, M.; van Rossum, B.; de Groot, H.; Oschkinat, H. *ChemBioChem* **2001**, *2*, 272–281.
- (76) Igumenova, T. I.; McDermott, A. E.; Zilm, K. W.; Martin, R. W.; Paulson, E. K.; Wand, A. J. *J. Am. Chem. Soc.* **2004**, *126*, 6720–6727.
- (77) Bockmann, A. *Compt. Rend. Chim.* **2006**, *9*, 381–392.
- (78) Ulrich, E. L.; Akutsu, H.; Doreleijers, J. F.; Harano, Y.; Ioannidis, Y. E.; Lin, J.; Livny, M.; Mading, S.; Maziuk, D.; Miller, Z.; et al. *Nucleic Acids Res.* **2008**, *36*, D402–408.
- (79) Wang, Y. J.; Jardetzky, O. *Protein Sci.* **2002**, *11*, 852–861.
- (80) Bax, A.; Freeman, R.; Kempshall, S. P. *J. Am. Chem. Soc.* **1980**, *102*, 4849–4851.
- (81) Cadars, S.; Sein, J.; Duma, L.; Lesage, A.; Pham, T. N.; Baltisberger, J. H.; Brown, S. P.; Emsley, L. *J. Magn. Reson.* **2007**, *188*, 24–34.
- (82) Grasso, G.; de Swiet, T. M.; Titman, J. *J. Phys. Chem. B* **2002**, *106*, 8676–8680.
- (83) Sergeyev, I.; Day, L. A.; Goldbourt, A.; McDermott, A. E. *J. Am. Chem. Soc.* **2011**, In press.
- (84) Ryutaro, O.; Takegoshi, K. *J. Chem. Phys.* **2006**, *125*, 214503.
- (85) Marvin, D. A.; Welsh, L. C.; Symmons, M. F.; Scott, W. R. P.; Straus, S. K. *J. Mol. Biol.* **2006**, *355*, 294–309.
- (86) Wang, Y. A.; Yu, X.; Overman, S.; Tsuboi, M.; Thomas, J. G. J.; Egelman, E. H. *J. Mol. Biol.* **2006**, *361*, 209–215.
- (87) Zimmermann, K.; Hagedorn, H.; Heuck, C. C.; Hinrichsen, M.; Ludwig, H. *J. Biol. Chem.* **1986**, *261*, 1653–1655.
- (88) Tang, J.; Fraden, S. *Liq. Cryst.* **1995**, *19*, 459–467.